Electronic Supplementary Information

Flexible keratin hydrogels obtained by a reductive method

María Luz Peralta Ramos,[a,b] Patricia Rivas-Rojas,[c,d] Hugo Ascolani,[e] Margherita Cavallo,[f] Francesca Bonino,[f] Roberto Fernandez de Luis,[g] María Ximena Guerbi,[h] Flabia Michelini,[h] Celina Bernal,[i] Juan Manuel Lázaro-Martinez,[a,b] and Guillermo Copello*[a,b]

[a]Universidad de Buenos Aires. Facultad de Farmacia y Bioquímica. Departamento de Ciencias Químicas. Buenos Aires, Argentina
[b]CONICET - Universidad de Buenos Aires. Instituto de Química y Metabolismo del Fármaco (IQUIMEFA). Buenos Aires, Argentina
[c]Instituto de Tecnologías Emergentes y Ciencias Aplicadas (ITECA), UNSAM-CONICET, Escuela de Ciencia y Tecnología, Laboratorio de Cristalografía Aplicada, San Martín, Buenos Aires, Argentina
[d]Instituto de Materiales y Procesos Termomecánicos, Universidad Austral de Chile, Valdivia, Chile
[e]Centro Atómico Bariloche, CNEA y CONICET, R8402AGP Bariloche, Argentina
[f]Department of Chemistry, NIS and INSTM Reference Centers, Università di Torino, Via P. Giuria 7, I-10125 Torino and Via G. Quarello 15/A, I-10135, Torino, Italy.
[g]BCMaterials, Basque Center for Materials, Applications and Nanostructures, UPV/EHU Science Park, 48940 Leioa, Spain
[h]Centro de Medicina Traslacional, Hospital de Alta Complejidad El Cruce Néstor Kirchner, Buenos Aires, Argentina.
[i]Grupo de Ingeniería en Polímeros y Materiales Compuestos, Instituto de Tecnología en Polímeros y Nanotecnología (ITPN-UBA-CONICET), Facultad de Ingeniería, Universidad de Buenos Aires, Las Heras 2214 (CP 1127AAR), Buenos Aires, Argentina

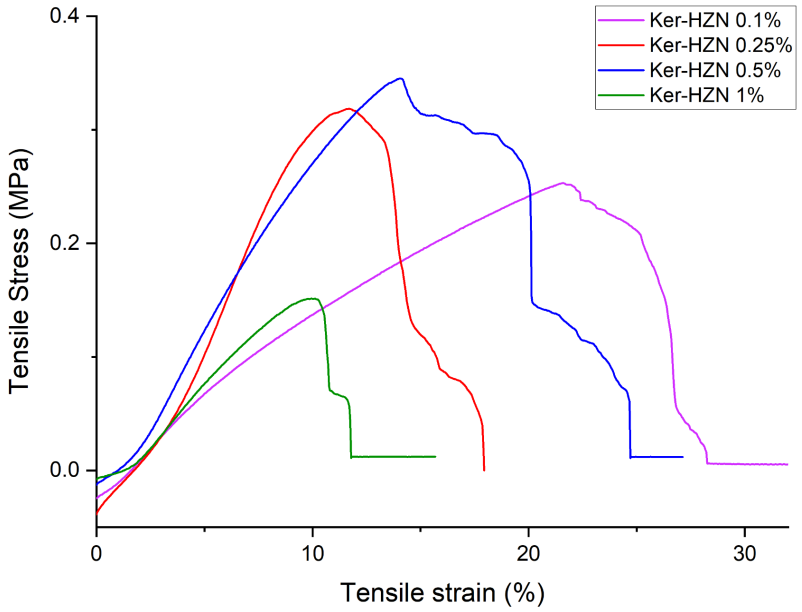

Figure S1. *Mechanical behaviour of Ker-HZN hydrogels.*

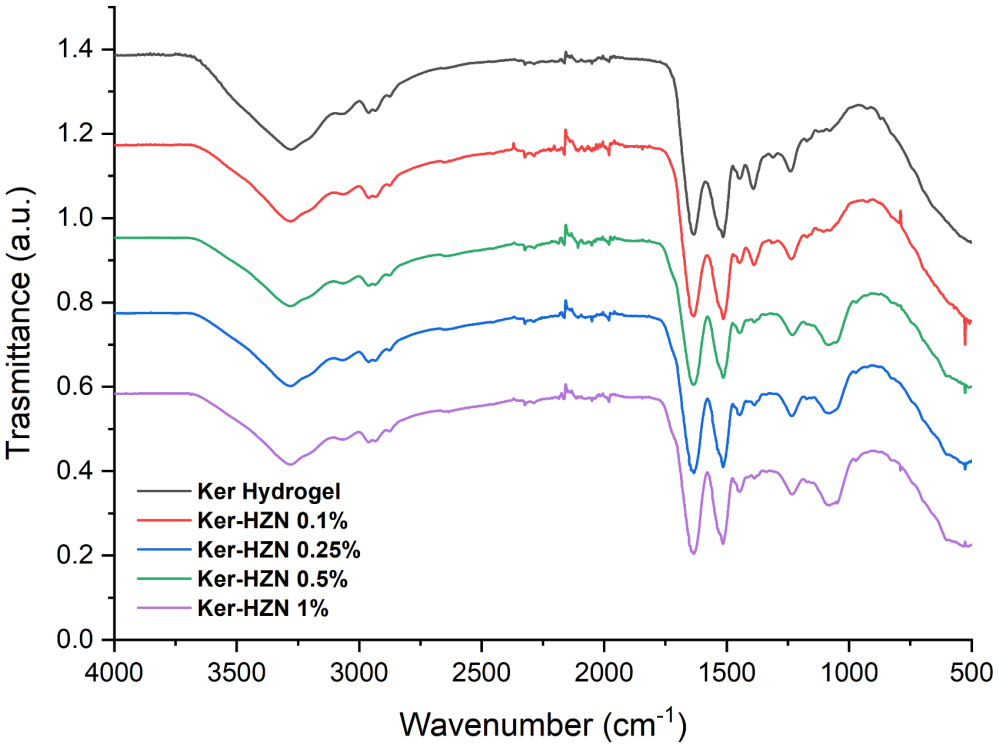

Figure S2. *Full FT-IR spectra of Ker and Ker-HZN x% hydrogels.*

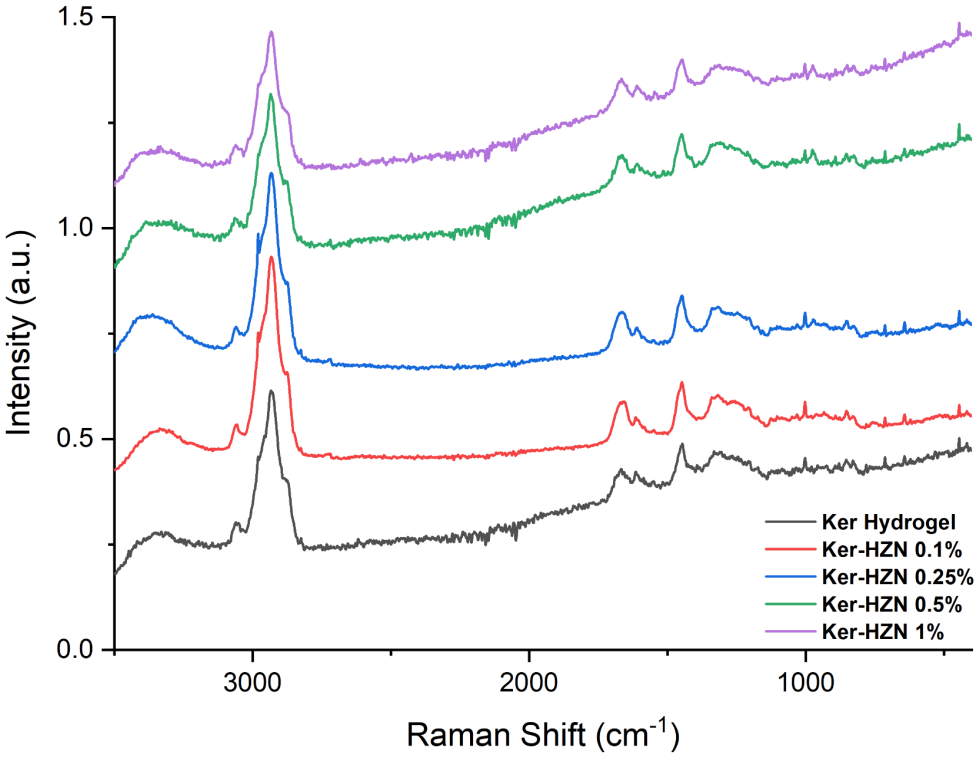

Figure S3. *Full Raman spectra of Ker and Ker-HZN x% hydrogels.*

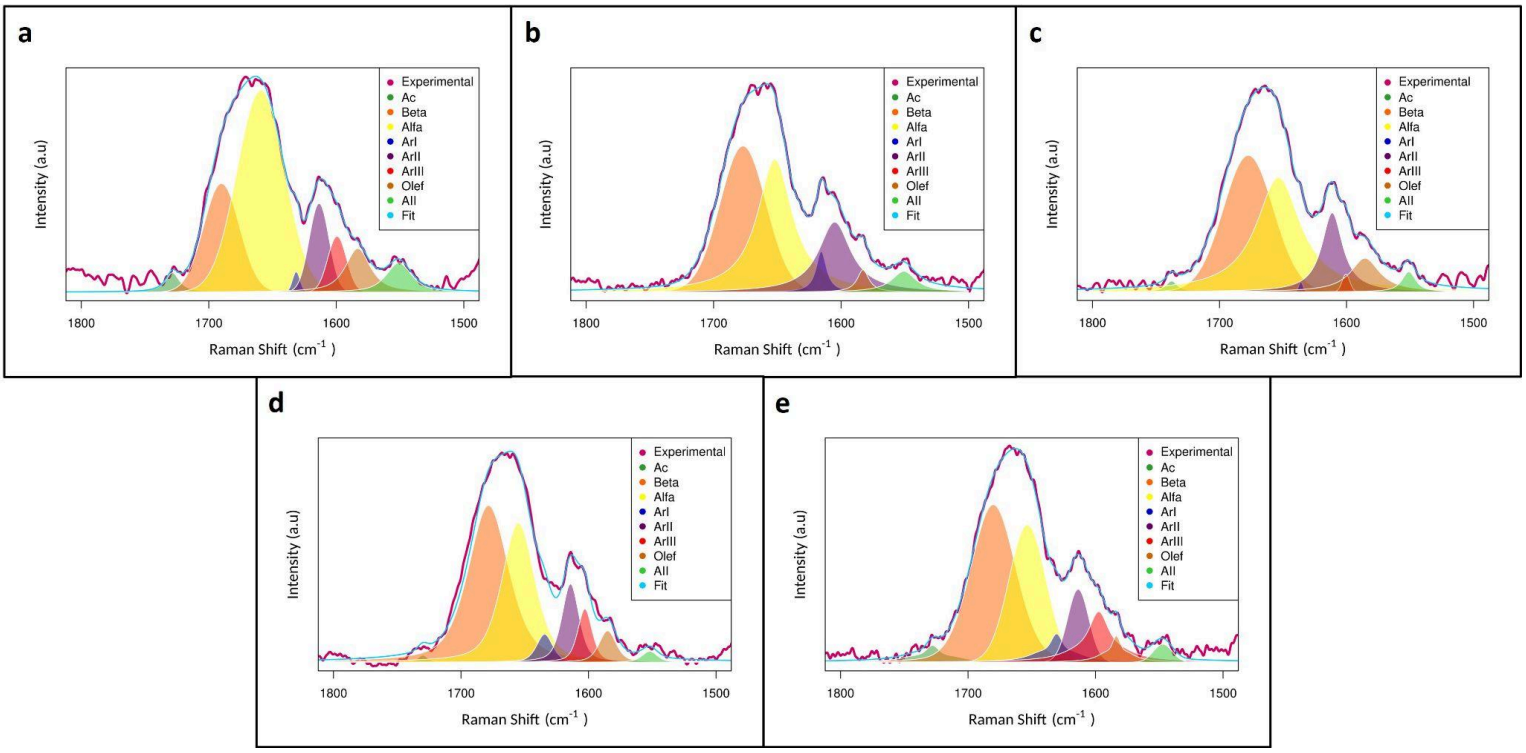

Figure S4. *Deconvolution of Raman Amide I peak of a) Keratin hydrogel, b) Ker-HZN 0.1%, c) Ker-HZN 0.25%, d) ker-HZN 0.5% and e) Ker-HZN 1%.*

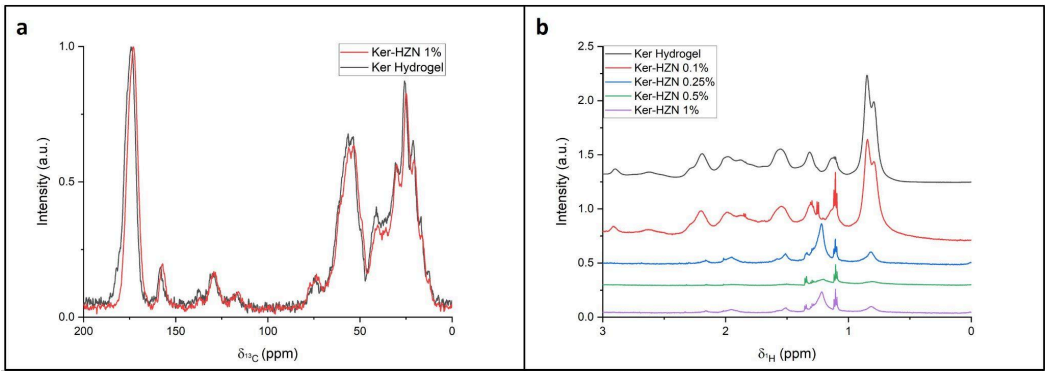

Figure S5. *a) Solid-state ^{13}C CP-MAS NMR, b) ^{1}H HRMAS-NMR spectra of Ker and Ker-HZN x% hydrogels.*

XPS analysis

The samples (in powder form) were attached to stainless steel sample holders using double-sided conductive carbon tape. All the analysed samples showed significant surface charge effects with X-ray irradiation. A typical wide-scan spectrum is shown in Figure S4. Special care was taken during data acquisition of the detailed core-level spectra in order to handle these effects. Concretely, the following procedure was applied systematically: multiple partial spectra were measured and, between them, the binding-energy (BE) position of the N1s peak was monitored. Finally, assuming that the position of the N1s peak should be constant during the measurement, the recorded partial core-level spectra were aligned and summed.

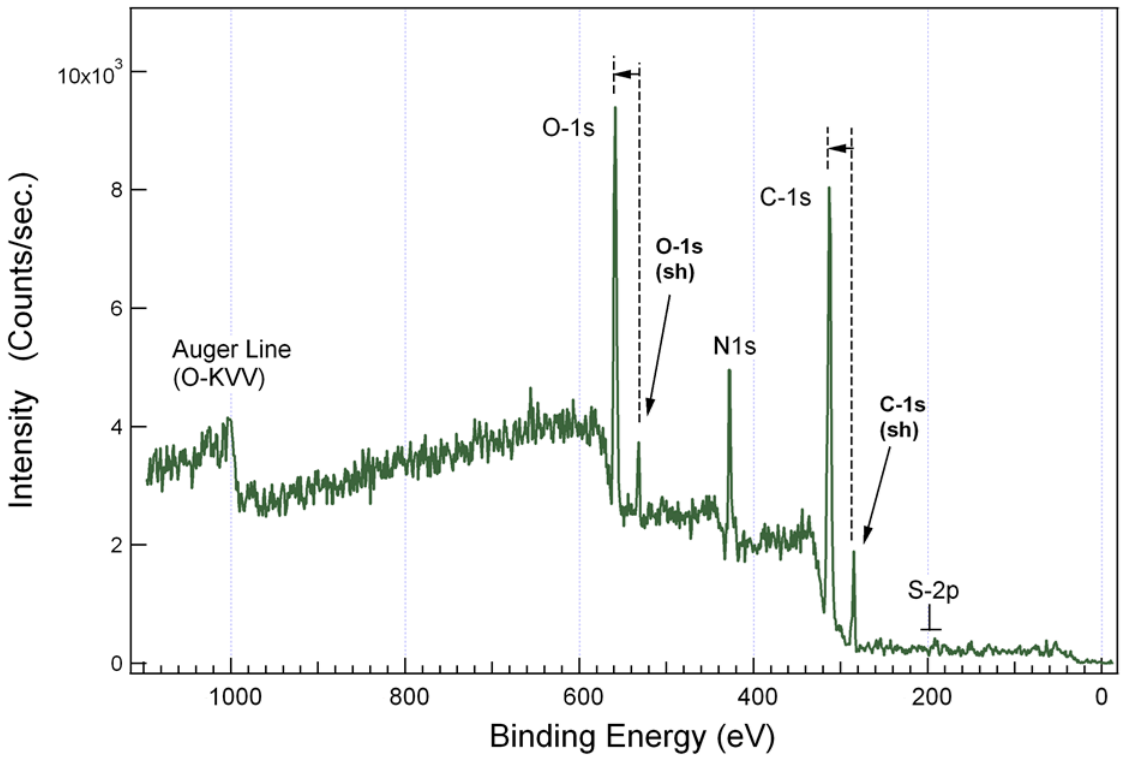

Figure S6: *Typical wide-scan XPS spectrum obtained from the analysed keratin samples.*

Four chemical elements, namely O, N, C, S, are consistently observed as expected for a keratin molecule. In addition to the sample-associated peaks, C1s and O1s peaks originating from the sample holder (sh) are often observed at BE ~285 and ~532 eV, respectively. In the particular case, those peaks originating from the sample appear shifted towards higher BE due to the effects of surface charge induced by X-radiation. Note that these charge effects caused a separation of the C1 and Os signals coming from the sample from those coming from the sample holder.

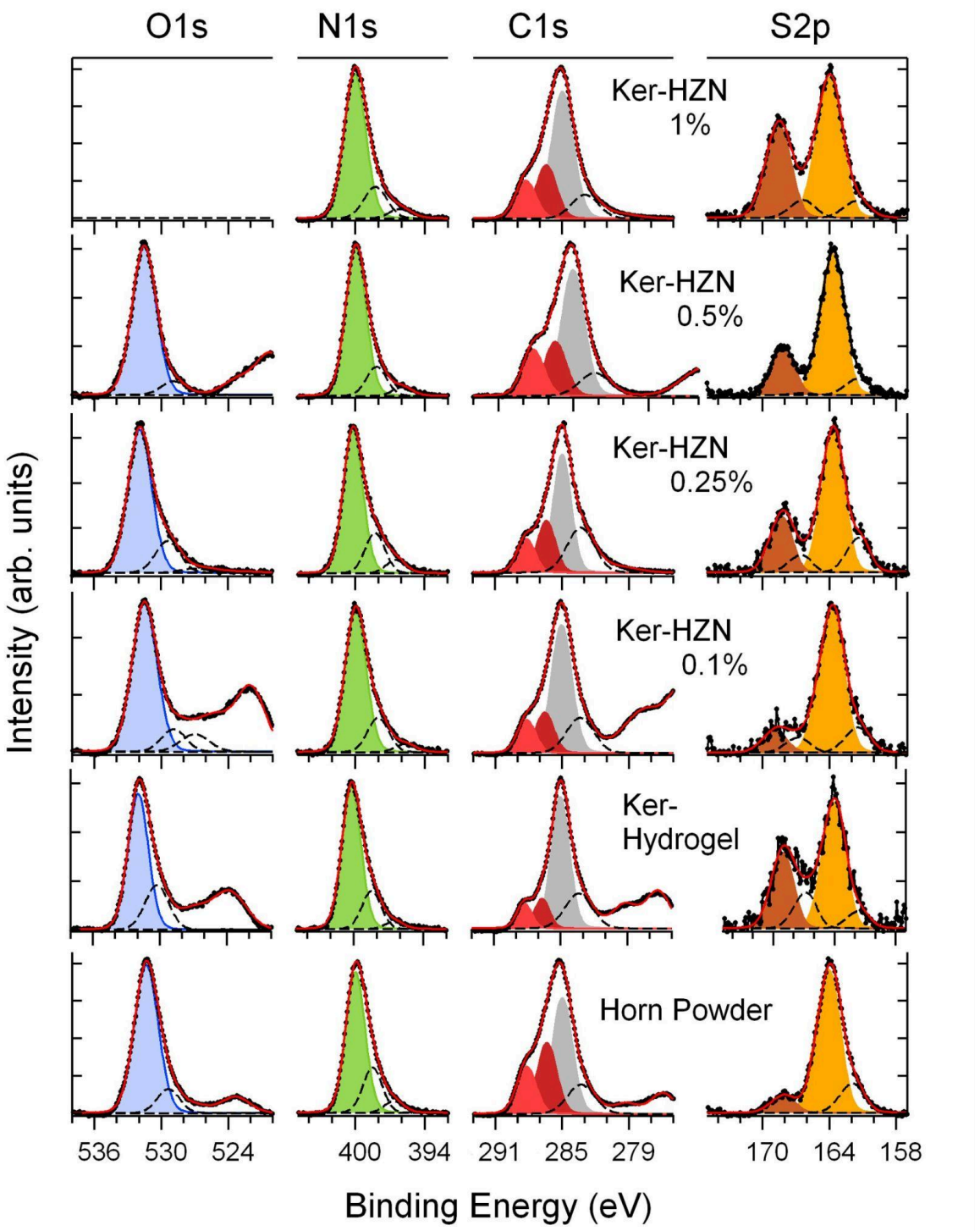

Figure S7: *XPS spectra of keratin samples illustrating the effects of different treatments with hydrazine.*

From bottom to top, each row corresponds to the following: cow-horn powder, keratin hydrogel, and keratin hydrogel treated with hydrazine at different concentrations (HZN x%). Each experimental spectrum (black dots) is accompanied by the results of its fit analysis. All the spectra are normalized to their maximum intensity.

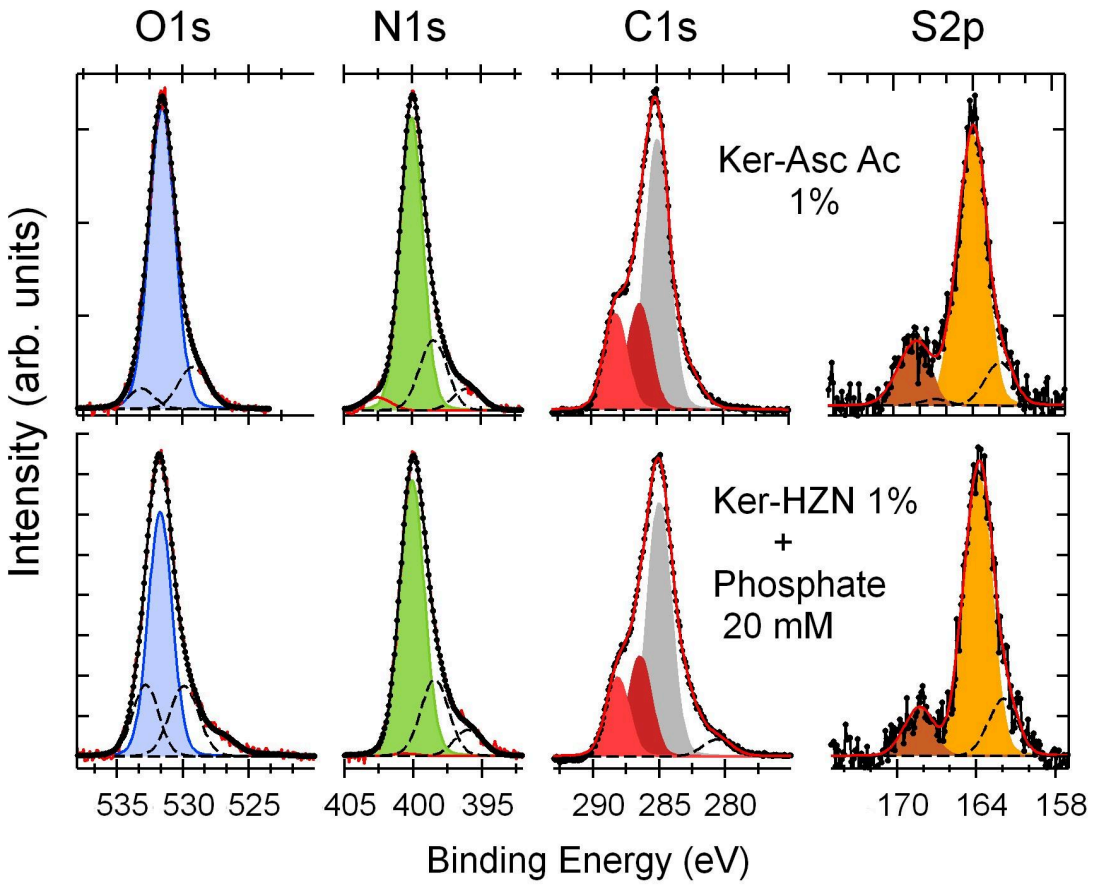

Figure S8: *XPS spectra of keratin samples illustrating the effects of applying a buffer solution after a treatment with 1% hydrazine (bottom row), and of the treatment of ker-hydrogel with ascorbic acid 1% (top row).*

Each experimental spectrum (black dots) is accompanied by the results of its fit analysis. All the spectra are normalized to their maximum intensity. In some samples (hydrogel, HZN-0.1% and HZN-0.5%), the effect of surface charge is relatively small and, for this reason, the C1s and O1s peaks originating from the sample appear close to those from the sample holder causing the structures observed on the low-BE side of the O1s and C1s spectra.

For each spectrum, the components considered in our analysis (coloured) are those that appear systematically in all the samples analysed and can be assigned to a specific origin. Additional components (black dashed lines) were included in the fit to account for asymmetries in the spectra that are probably due to the fact that the surface charge is not homogeneous. They do not always appear and do not have a specific assignment.

Table S1: Summary of the BE positions of the relevant components corresponding to the fits shown in Figure S5 and S6.

Sample	O1s	N1s	C1s			S2p		[S]/[N]
			C2	C1	C0	S2	S1	
Horn Powder	531.37	400.02	288.23	286.39	285.0	167.80	163.72	0.083
Ker Hydrogel	531.96	400.23	288.29	286.67	285.0	168.79	163.73	0.054
Ker-HZN 0.1%	531.53	400.00	288.21	286.58	285.0	168.58	163.47	0.048
Ker-HZN 0.25%	531.91	400.21	288.23	286.41	285.0	168.03	163.44	0.055
Ker-HZN 0.5%	531.56	399.98	288.23	286.46	285.0	167.87	163.41	0.062
Ker-HZN 1%		400.06	288.30	286.45	285.0	168.27	163.67	0.077
Ker-HZN 1% + Phosphate Buffer	531.72	400.10	288.17	286.34	285.0	168.00	163.58	0.046
Ker Hydrogel + Ascorbic Acid 1%	531.57	400.07	288.16	286.46	285.0	168.06	163.75	0.049
Average values	531.66	400.08	288.22	286.48	285.0	168.17	163.68	

The main peak in the C1s spectrum is assigned to C adventitia and placed at 285 eV to define the zero of the energy scale in each sample. The other two peaks in the C1s spectrum, which appear consistently around -286.5 and -288.2 eV and with similar intensities, are respectively assigned to C atoms in C-N bonds (C1) and C atoms in C-O bonds (C2). The main peak in the N1s spectrum consistently appears around -400.1 eV, which is consistent with N atoms in N-HC2 bonds. The two peaks in the S2p spectrum, which appear consistently around 163.7 and 168.2 eV, are assigned to S atoms in S-S or S-H bonds (S1) and S atoms in S-O bonds (S2). The last column on the right of Table S1 summarizes the sulphur concentrations [S] relative to that of nitrogen [N] derived from the spectra shown in Figures S5 and S6. These values were obtained by dividing the full area of a given experimental S2p spectrum (after subtracting background) by the full area of the corresponding N1s spectrum, and correcting both areas by the corresponding photoionization cross-sections.

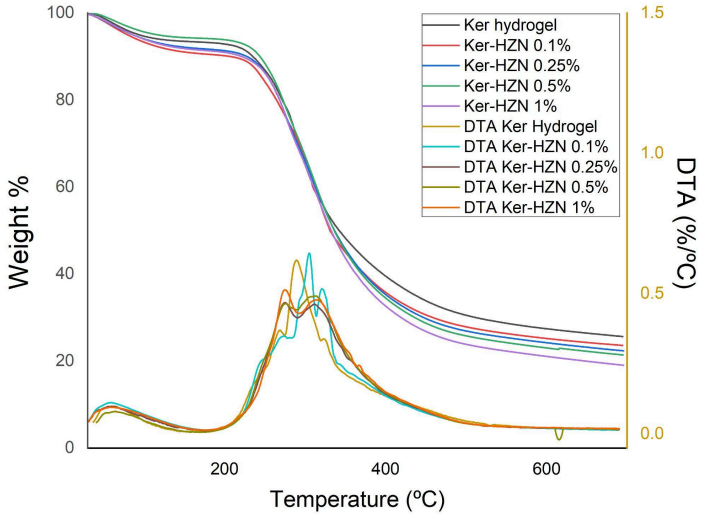

Figure S9: DTA and TGA thermogram of Ker, Ker-HZN x% hydrogels.

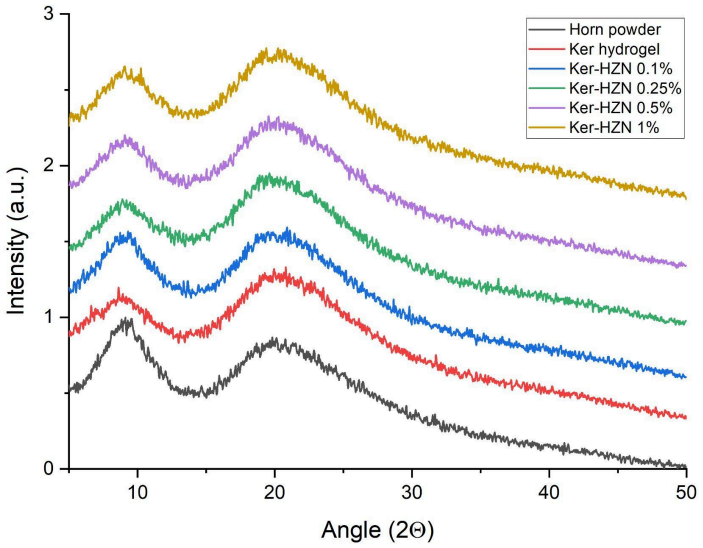

Figure S10. XRD diffractograms of Ker, Ker-HZN x% hydrogels.

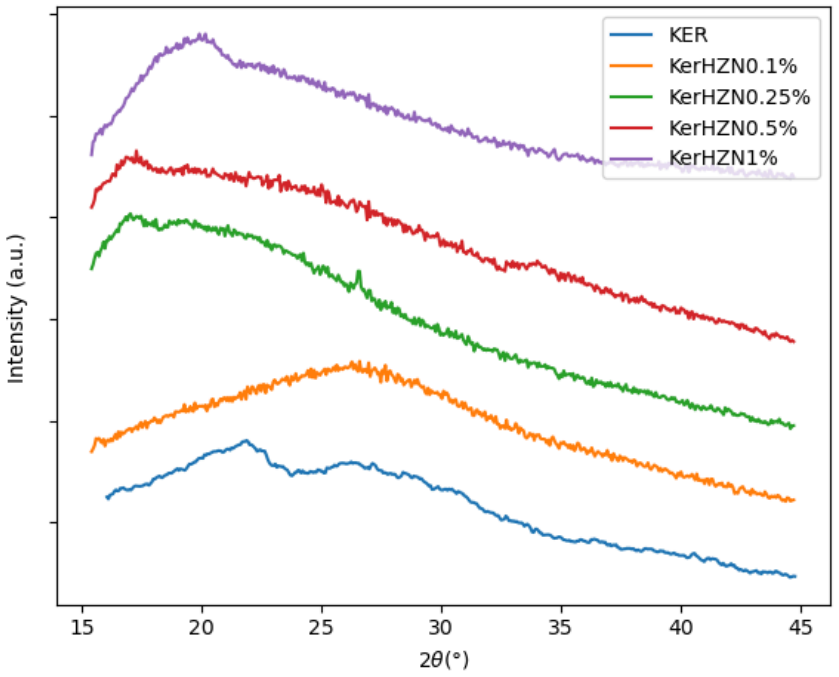

Figure S11. WAXS profiles of Ker and Ker-HZN x% hydrogels.

SAXS patterns analysis models

Swollen pores approach (Two-phase model) For the analysis of the patterns, a plugin model combining two pre-existing models was computed in SASView software.[1] On one hand, a power law to account for the scattering of the mass fractals like behavior of the entangled filaments, related to the low *q* region. And on the other, a Guinier-Porod (GP) function,[2] related to the scattering of the pores formed by the polymer network, displayed in the patterns as a “bump” in the mid-to-high *q* range. Given the complexity of the system, in

the GP function the dimension variable and the Porod exponent were constrained to 0 and 3 respectively, assuming as a first approximation spherical pores of rather rough surfaces. Yielding the following expression for the intensity:

$$I(q)=\frac{A}{q^n}+\begin{cases} B\exp\left(\frac{-q^2 R_g^{\,2}}{3}\right) & q\le q_1 \\ \frac{C}{q^3} & q\ge q_1 \end{cases}$$

with

$$q_1=\frac{1}{R_g}\sqrt{\frac{9}{2}}\wedge C=\frac{1}{R_g^{\,3}}\exp\left[\frac{-3}{2}\right]\left(\frac{9}{2}\right)^{\frac{3}{2}}$$

Where the continuity of the Guinier and Porod function and their derivatives is enforced. Further information about these functions can be found in the SASView documentation.

Here *Rg* is a parameter related to the size of the pores (assuming spherical pores *Rg* =*R*√3/5), and n can be related to the “openness” of the structure as a consequence of swelling, going from a clustered network when *n*=3 to a swollen structure when *n*=5/3.

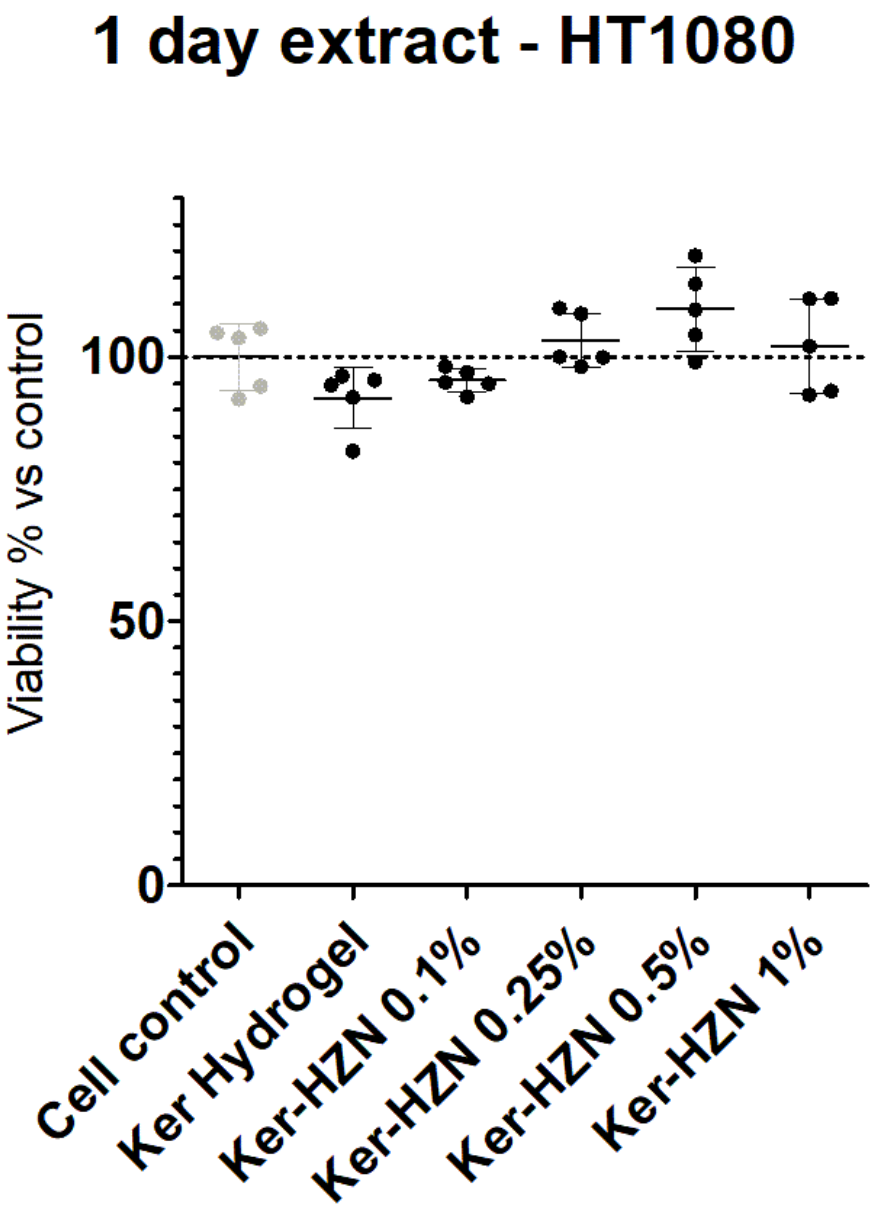

Figure S12. MTT assay of Ker Hydrogel and Ker-HZN x % using HT1080 cell line.

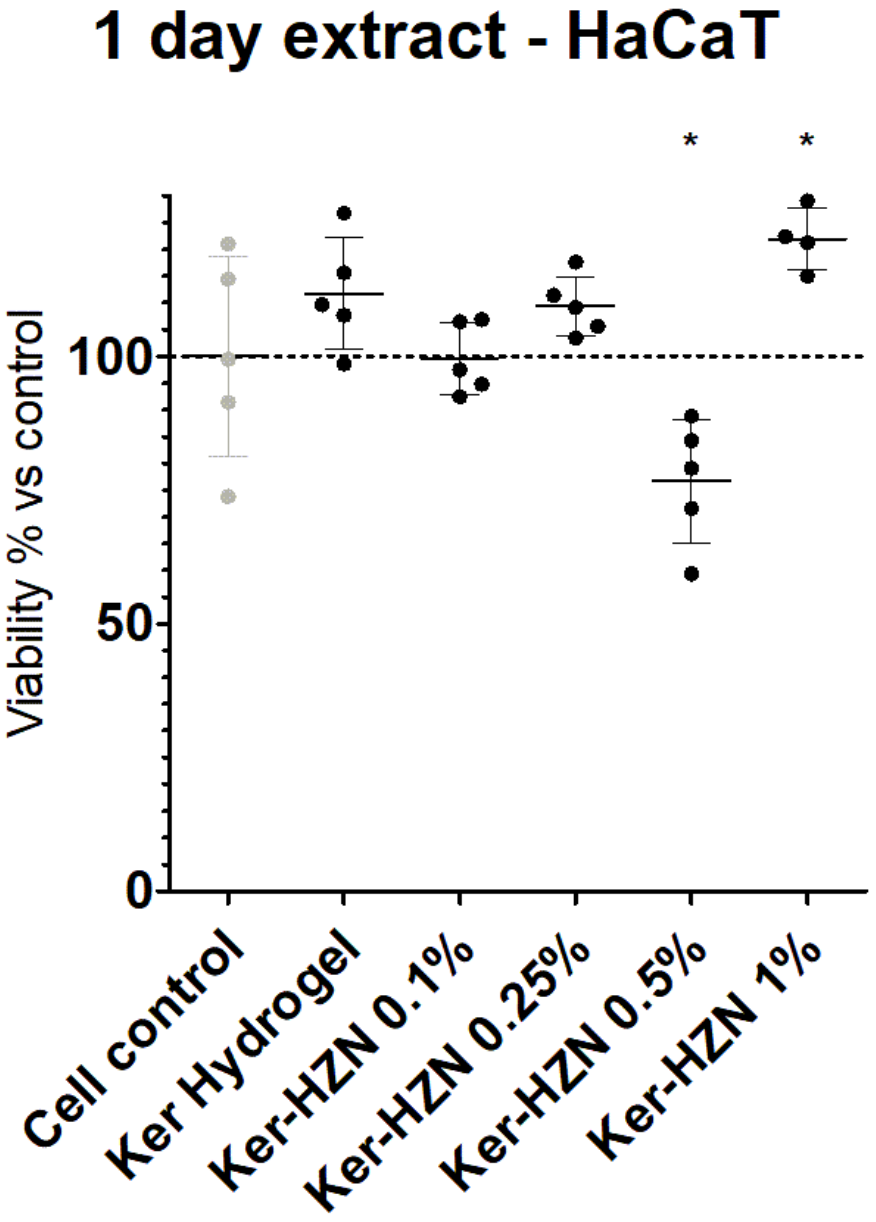

Figure S13. MTT assay of Ker Hydrogel and Ker-HZN x % using HaCaT cell line.

References

1 guinier_porod — SasView 5.0.5 documentation, https://www.sasview.org/docs/user/models/guinier_porod.html?highlight=guinier+porod, (accessed 26 June 2023).
2 B. Hammouda, *J. Appl. Crystallogr.*, 2010, **43**, 1474–1478.